PCCP

COMMUNICATION

View Article Online
View Journal | View Issue

Cite this: *Phys. Chem. Chem. Phys.*, 2018, **20**, 17557

Received 24th April 2018,
Accepted 7th June 2018

DOI: 10.1039/c8cp02616e

rsc.li/pccp

Binary mixtures of charged colloids: a potential route to synthesize disordered hyperuniform materials

Duyu Chen,[a] Enrique Lomba [ab] and Salvatore Torquato *[acde]

Disordered hyperuniform materials are a new, exotic class of amorphous matter that exhibits crystal-like behavior, in the sense that volume-fraction fluctuations are suppressed at large length scales, and yet they are isotropic and do not display diffraction Bragg peaks. These materials are endowed with novel photonic, phononic, transport and mechanical properties, which are useful for a wide range of applications. Motivated by the need to fabricate large samples of disordered hyperuniform systems at the nanoscale, we study the small-wavenumber behavior of the spectral density of binary mixtures of charged colloids in suspension. The interaction between the colloids is approximated by a repulsive hard-core Yukawa potential. We find that at dimensionless temperatures below 0.05 and dimensionless inverse screening lengths below 1.0, which are experimentally accessible, the disordered systems become effectively hyperuniform. Moreover, as the temperature and inverse screening length decrease, the level of hyperuniformity increases, as quantified by the "hyperuniformity index". Our results suggest an alternative approach to synthesize large samples of effectively disordered hyperuniform materials at the nanoscale under standard laboratory conditions. In contrast with the usual route to synthesize disordered hyperuniform materials by jamming particles, this approach is free from the burden of applying high pressure to compress the systems.

The concept of disordered hyperuniformity was first introduced in the context of many-particle systems over a decade ago,[1] and was subsequently generalized to two-phase heterogeneous materials.[2] Disordered hyperuniform systems and materials belong to a new, exotic class of amorphous matter that lies between crystal and fluid states: they behave like crystals in the way that they suppress density or volume-fraction fluctuations at large length scales, and yet they are statistically isotropic with no Bragg diffraction peaks, as in the case of liquids or glasses.[3] Specifically, for disordered hyperuniform materials, the local volume-fraction variance $\sigma_V^2(R)$ within a d-dimensional spherical observation window of radius R approaches zero for large R asymptotically more rapidly than the inverse of the window volume, *i.e.*, faster than R^{-d}.[2] This is different from typical disordered two-phase materials, which possess $\sigma_V^2(R)$ that vanishes like R^{-d} for large R. Equivalently, the spectral density $\tilde{\chi}_V(k)$, which is proportional to the scattering intensity, approaches zero as the wavenumber k vanishes,[2,4] *i.e.*,

$$\lim_{k\to 0} \tilde{\chi}_V(k) = 0. \tag{1}$$

Note that the widely used structure factor $S(k)$ can be thought of as the counterpart of $\tilde{\chi}_V(k)$ for point patterns.[5] Methods to design realizations of two-phase disordered hyperuniform systems have been devised.[6–8]

Disordered hyperuniform systems have been shown to be endowed with novel physical properties; see the recent overview by Torquato.[3] In particular, disordered hyperuniform dielectric networks were found to possess large complete photonic band gaps comparable in size to photonic crystals, but superior to photonic crystals because of their perfect isotropy and robustness to defects.[9,10] As a result, these networks are suitable for a wide range of applications such as lasers, sensors, waveguides, and optical microcircuits. Similarly, disordered hyperuniform materials possess desirable phononic, electronic, transport, and mechanical properties, and wave-propagation characteristics,[6,7,11–19] and their full potential in technological applications has yet to be explored.

Despite the desirable physical properties and technological potential of disordered hyperuniform materials, their synthesis and fabrication remain challenging, especially for large samples at the nanoscale. While 3D printing and lithographic technologies can now be applied to the rational design of materials with tunable disorder at the micro-scale,[6,8,20] in this particular instance, the

[a] *Department of Chemistry, Princeton University, Princeton, New Jersey 08544, USA. E-mail: torquato@electron.princeton.edu*
[b] *Instituto de Química Física Rocasolano, CSIC, Calle Serrano 119, E-28006 Madrid, Spain*
[c] *Department of Physics, Princeton University, Princeton, New Jersey 08544, USA*
[d] *Princeton Institute for the Science and Technology of Materials, Princeton University, Princeton, New Jersey 08544, USA*
[e] *Program in Applied and Computational Mathematics, Princeton University, Princeton, New Jersey 08544, USA*

spatial resolution of these techniques limits their application at the nanoscale. Novel avenues need to be explored to optimize fabrication in the nanometer range.

The self-assembly and self-structuring of nanoparticles with designed interactions into target structures represents a promising route,[21,22] and its application to the synthesis of disordered hyperuniform materials is still in its infancy. While disordered hyperuniformity was shown to arise in hard-particle systems as they approach jammed (mechanically stable) states,[23–25] the experimental realization of such systems requires applying high pressure to compress the systems, which is challenging. It is also known that systems with pure Coulombic interactions in a neutralizing background can be disordered and hyperuniform at positive temperatures.[26–28] However, these systems by themselves cannot be experimentally realized. Any real charged colloidal systems will have a finite non-zero inverse screening length for a finite non-zero counterion concentration, by which $\tilde{\chi}_V(k = 0)$ will also be non-zero.

In this work, as an alternative, we computationally explore the use of the self-structuring (self-assembly) process of binary mixtures of charged colloids in suspension in order to guide experimentalists to fabricate large samples of effectively disordered hyperuniform materials in two dimensions. Specifically, it is desirable that these designed materials be realized in the laboratory at the nanoscale without resorting to compression techniques. Following the coarse-graining approach of Derjaguin, Landau, Verwey and Overbeek[29,30] (DLVO), we model the colloidal particles using repulsive hard-core Yukawa interactions.[31,32] The system is studied by means of canonical Monte Carlo simulations, using a sample size, N, of 10 000 particles and periodic boundary conditions. We note that this system size is already large enough to determine the small-k behavior of the systems given the range of our potential, and it is reasonable to assume that the effective disordered hyperuniformity will also hold for large sample sizes and thus could be realized in experiments. We have considered different systems with varying inverse screening lengths (*i.e.*, effective counterion concentrations in the DLVO model) and temperatures, up to a total of 50 different systems and conditions. Particle size disparity is introduced to frustrate crystallization.[25] Our two-dimensional study is applied to particles at interfaces and thin films (monolayers). Additionally, for a periodic finite sample, in two dimensions we can access smaller wavenumbers with a scaling of $2\pi/\sqrt{N}$, compared to the scaling of $2\pi/N^{1/3}$ in three dimensions. We study the small-k behavior of the volume-fraction fluctuations of the resulting structures, as measured by the spectral density. To that aim we employ the "hyperuniformity index", H, defined as:

$$H = \tilde{\chi}_V(0)/\tilde{\chi}_V(k = k_{max}), \quad (2)$$

where $\tilde{\chi}_V(0)$ is the extrapolated value of the spectral density as k approaches zero and $\tilde{\chi}_V(k = k_{max})$ is the value of the largest peak (often the first peak) of the spectral density. Clearly, the lower is the value of H, the larger the degree of hyperuniformity displayed by the system. In this work, we deem the systems to be effectively hyperuniform whenever $H \leq 10^{-2}$, consistent with previous experiences concerning hyperuniformity in binary maximally-randomly-jammed packings of hard disks.[25] However, as detailed below, we note that H here is different from its counterpart H_S based on the structure factor that is used in previous works.[25,33,34]

We find that at experimentally accessible temperatures and inverse screening lengths, the disordered structures indeed become effectively hyperuniform. Moreover, the degree of hyperuniformity, as measured by H, increases as the temperature and inverse screening lengths decrease. On the other hand, the spatial distribution associated with each individual component is not hyperuniform, *i.e.*, the system is not "multihyperuniform" (the patterns of both the total population and the individual types are simultaneously hyperuniform),[35] which is in contradistinction to some systems with bare Coulomb interactions.[28]

The hard-repulsive Yukawa potential between particles i and j is given by[31,32]

$$v(r_{ij}) = \begin{cases} \infty, & r_{ij} \leq D_{ij} \\ \varepsilon_{ij}\left(\dfrac{\exp[-\kappa(r_{ij} - D_{ij})]}{r_{ij}/D_{ij}} - \dfrac{\exp[-\kappa(r_C - D_{ij})]}{r_C/D_{ij}}\right), & D_{ij} \leq r_{ij} \leq r_C \\ 0, & r_{ij} > r_C \end{cases} \quad (3)$$

where r_{ij} is the distance between particles i and j, $D_{ij} = R_i + R_j$ (R_i and R_j are the hard-core radii of particles i and j), κ is the inverse screening length, and r_C is the cutoff of the soft repulsions [chosen to be sufficiently large compared to the screening length, which increases as the screening length increases such that the cutoff does not affect $\tilde{\chi}_V(0)$]. The energy of the system E is the sum of these effective pairwise repulsions, *i.e.*,

$$E = \sum_{i<j} v(r_{ij}). \quad (4)$$

Here we consider an equimolar binary mixture of small and large colloids with a small to large colloid diameter ratio $\alpha \equiv D_S/D_L = 2/3$ and a small-colloid mole fraction $x \equiv N_S/(N_S + N_L) = 0.5$. The packing fraction (the fraction of space covered by the colloids) is set to $\phi = 0.21$. Here D_S and D_L are the hard-core diameters of the small and large colloids, and N_S and N_L are the number of small and large colloids in the system, respectively. We set the ratios of the energy scales to $\varepsilon_{SS} : \varepsilon_{SL} : \varepsilon_{LL} = 1 : 2 : 4$, where ε_{SS}, ε_{SL}, and ε_{LL} are energy scales of the interactions between two small colloids, between a small colloid and a large colloid, and between two large colloids, respectively. In addition, we note that the behavior of our systems at small wavenumbers is not sensitive to the specific choice of the values of D_S/D_L, N_S/N_L, and $\varepsilon_{SS} : \varepsilon_{SL} : \varepsilon_{LL}$.

We then systematically study the effect of temperature T and the inverse screening length κ on the small-k behavior of the spectral density of our system. For each T and κ, we employ a standard canonical Monte Carlo simulation technique.[36,37] After a thermalization run consisting of 5000 translation trials per particle, we collect 50 uncorrelated sample configurations from each system and temperature under consideration. The pair

structure is first analyzed in terms of the total pair correlation function, $g_2(r)$, and the corresponding spectral density, $\tilde{\chi}_V(k)$. Specific contributions for each mixture component are also studied. Thus, for a binary mixture of small and large colloidal particles, $g_2(r)$ can be decomposed into three components:

$$g_2(r) = x^2 g_{2,S}(r) + (1 - x)^2 g_{2,L}(r) + 2x(1 - x)g_{2,C}(r), \quad (5)$$

where x is the small colloid relative concentration, $g_{2,S}(r)$ and $g_{2,L}(r)$ are the pair distribution functions of the small and large colloids, respectively, and $g_{2,C}(r)$ is a cross-correlation term. In parallel, the spectral density $\tilde{\chi}_V(k)$ can be decomposed into three contributions:

$$\tilde{\chi}_V(k) = \tilde{\chi}_{V,S}(k) + \tilde{\chi}_{V,L}(k) + \tilde{\chi}_{V,C}(k), \quad (6)$$

where $\tilde{\chi}_{V,S}(k)$, $\tilde{\chi}_{V,L}(k)$, and $\tilde{\chi}_{V,C}(k)$ are given by

$$\tilde{\chi}_{V,S}(k) = \frac{\left|\tilde{m}(k; R_S)\sum_{j=1}^{N_S}\exp\left(-i\mathbf{k}\cdot\mathbf{r}_j^{(S)}\right)\right|^2}{V}, \quad (7)$$

$$\tilde{\chi}_{V,L}(k) = \frac{\left|\tilde{m}(k; R_L)\sum_{j=1}^{N_L}\exp\left(-i\mathbf{k}\cdot\mathbf{r}_j^{(L)}\right)\right|^2}{V}, \quad (8)$$

and

$$\tilde{\chi}_{V,C}(k) = 2\mathrm{Re}\left[\frac{\tilde{m}(k; R_S)\tilde{m}(k; R_L)\sum_{j=1}^{N_S}\exp\left(-i\mathbf{k}\cdot\mathbf{r}_j^{(S)}\right)\sum_{n=1}^{N_L}\exp\left(i\mathbf{k}\cdot\mathbf{r}_n^{(L)}\right)}{V}\right]. \quad (9)$$

Here $\tilde{\chi}_{V,S}(k)$ and $\tilde{\chi}_{V,L}(k)$ are the spectral densities of the small and large colloids, respectively, $\tilde{\chi}_{V,C}(k)$ is the cross-term (which already includes a factor two stemming from identical small–large and large–small contributions), $\{\mathbf{r}_j^{(S)}\}$ and $\{\mathbf{r}_n^{(L)}\}$ denote the positions of the small and large colloids, respectively, and $\tilde{m}(k;R)$ is the Fourier transform of the indicator function of a disk with radius R given by

$$\tilde{m}(k; R) = \frac{2\pi R}{k}J_1(kR). \quad (10)$$

where $J_1(x)$ is a Bessel function of the first kind. This quantity, which reflects the finite size of the particles, would correspond in a real scattering experiment to the form factor function, which accounts for the interaction of the probe particles (photons, electrons,...) with the individual sample particles.[38]

As an example, Fig. 1 shows a representative configuration of the equilibrated system with $\kappa D_S = 0.2$ at $k_BT/\varepsilon_{SS} = 0.1$, where k_B is the Boltzmann's constant. The lower graph corresponds to a 10-fold enlargement illustrating the size difference of our colloidal particles. Both figures correspond, at first sight, to a simple disordered fluid.

A more quantitative description at the pair-statistics level can be obtained from the computed total pair correlation function $g_2(r)$, and its three partial contributions, $g_{2,S}(r)$, $g_{2,L}(r)$, and $g_{2,C}(r)$. These are shown in Fig. 2, and are consistent

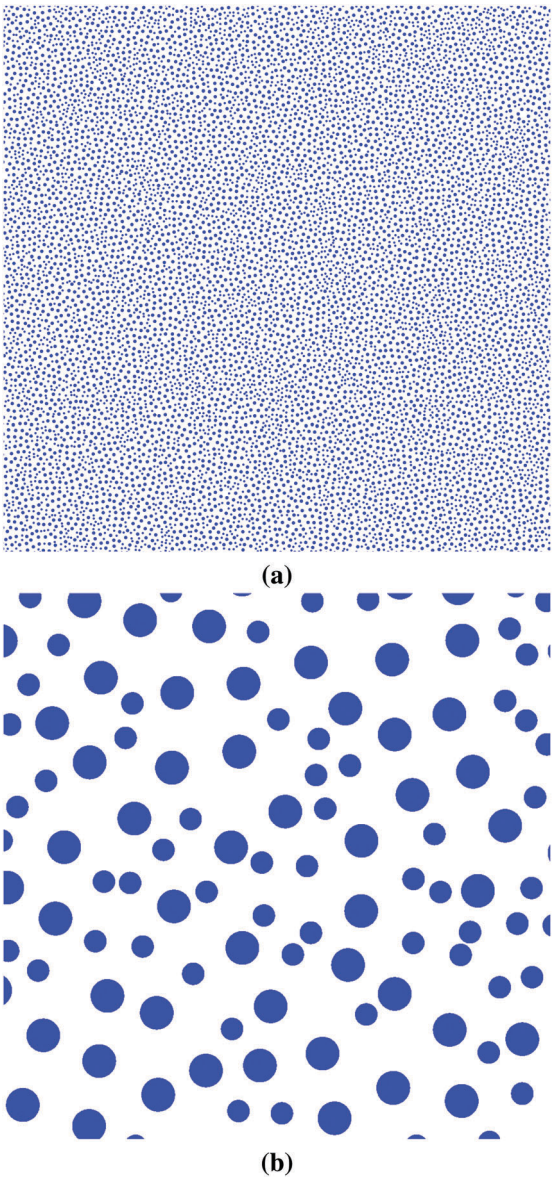

Fig. 1 (a) A representative configuration of the disordered effectively hyperuniform equilibrated equimolar mixture of large and small charged colloidal particles, with a small to large colloid diameter ratio α = 2/3, dimensionless inverse screening length κD_S = 0.2, a packing fraction ϕ of 0.21, and at dimensionless temperature k_BT/ε_{SS} = 0.1. (b) Zoomed-in region of a representative portion of the configuration depicted in (a).

with the apparent lack of long-range correlations, as can be appreciated by their decay to unity at pair distances $r \approx 5D_L$ and beyond in all instances.

The computed total spectral density $\tilde{\chi}_V(k)$ and its three components $\tilde{\chi}_{V,S}(k)$, $\tilde{\chi}_{V,L}(k)$, and $\tilde{\chi}_{V,C}(k)$ are shown in Fig. 3. We fit $\tilde{\chi}_V(k)$ with a third-order polynomial $f(k; a_0, a_1, a_2, a_3) = \sum_{j=0}^{n} a_j k^j$ for all wavenumbers within $0.0130 \leq kD_S/(2\pi) \leq 0.157$. Interestingly, the resulting intercept a_0 has a value of 2.26×10^{-3}, indicating that $\tilde{\chi}_V(k)$ effectively tends to zero as k approaches zero.

We have determined H to be 1.0×10^{-2} from the spectral density shown in Fig. 3, showing that the corresponding system

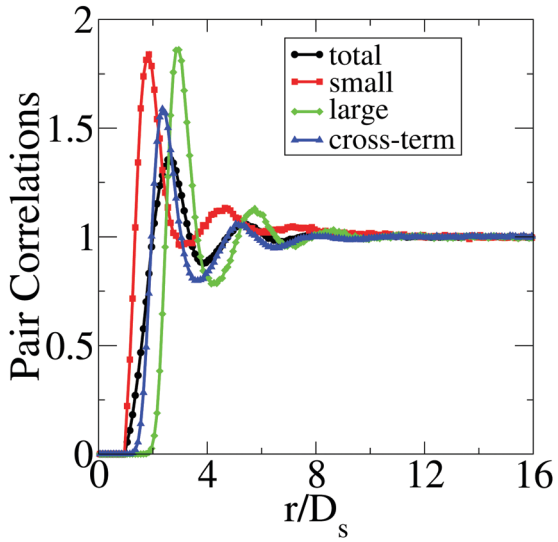

Fig. 2 Total pair correlation $g_2(r)$ and its partial counterparts for the small and large charged colloids and the cross-term $g_{2,S}(r)$, $g_{2,L}(r)$, and $g_{2,C}(r)$ of the equilibrated equimolar mixture of large and small charged colloidal particles, with a small to large colloid diameter ratio α = 2/3, dimensionless inverse screening length κD_S = 0.2, a packing fraction ϕ of 0.21, and at dimensionless temperature k_BT/ε_{SS} = 0.1. Note that all of these four pair correlation functions decay rapidly to unity as r increases, implying the lack of long-range order at the two-particle level for the overall system as well as the individual components.

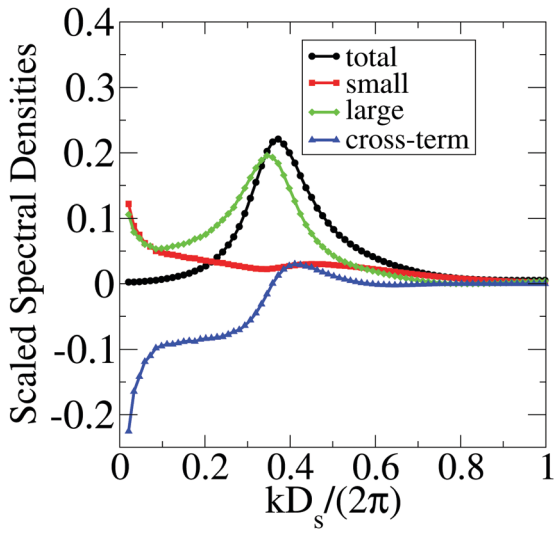

Fig. 3 Total spectral density $\tilde{\chi}_V(k)$ and its partial counterparts for the small and large colloids and the cross-term $\tilde{\chi}_{V,S}(k)$, $\tilde{\chi}_{V,L}(k)$, and $\tilde{\chi}_{V,C}(k)$ of the equilibrated equimolar mixture of large and small charged colloidal particles, with a small to large colloid diameter ratio α = 2/3, dimensionless inverse screening length κD_S = 0.2, a packing fraction ϕ of 0.21, and at dimensionless temperature k_BT/ε_{SS} = 0.1. Note that the spectral densities are all scaled by D_s^2 so that they are dimensionless, where D_s is the diameter of the small colloid. The total $\tilde{\chi}_V(k)$ practically vanishes as k approaches zero, implying the effective hyperuniformity of the overall system. However, this is not the case for the partial counterparts $\tilde{\chi}_{V,S}(k)$ and $\tilde{\chi}_{V,L}(k)$. This means that the spatial distributions of the small or large colloids alone are not hyperuniform, *i.e.*, the system is not "multihyperuniform".

is effectively hyperuniform. However, $\tilde{\chi}_{V,S}(k)$ and $\tilde{\chi}_{V,L}(k)$ do not tend to zero as k approaches zero, an indication that the spatial distribution of the small or large colloids alone is not "multihyperuniform".[35]

The value of H based on the spectral density $\tilde{\chi}_V(k)$ here is in general significantly higher than that of H_S based on the structure factor $S(k)$ of the corresponding point configurations [*i.e.*, $H_S = S(0)/S(k = k_{max})$, where $S(0)$ is the extrapolated value of $S(k)$ as k approaches zero and $S(k = k_{max})$ is its largest peak value]. For identical-particle packings, this is based on the fact that $\tilde{\chi}_V(k) = \rho\tilde{m}^2(k)S(k)$,[4,37] where $\tilde{m}(k)$ is the Fourier transform of the particle indicator function and ρ is the particle number density. Assuming that the location of the largest peak of $\tilde{\chi}_V(k)$ is roughly the same as that of $S(k)$, $H/H_S \approx \tilde{m}^2(0)/\tilde{m}^2(k_{max})$; since $\tilde{m}(k)$ achieves its maximum at $k = 0$ and $\tilde{m}^2(0) > \tilde{m}^2(k_{max})$, H should be higher than the corresponding H_S. For polydisperse packings, $\tilde{\chi}_V(k)$ possesses a prefactor similar to $\tilde{m}^2(k)$ that decreases H_S from H. We have, for example, computed here H and H_S for equilibrium monodisperse packing of hard disks at ϕ = 0.40, and find H to be 0.61 and H_S to be only 0.093. Also, as ϕ increases, the difference between H and H_S increases dramatically.

Next, we carry out a similar analysis for 50 different combinations of T and κ in the range of $k_BT/\varepsilon_{SS} \in [0.01,0.2]$ and $\kappa D_S \in [0.2,2.0]$. We then can construct a structural "phase diagram" of H in terms of T and κ, as shown in Fig. 4. Interestingly, H is on the order of 10^{-2}–10^{-3} when $k_BT/\varepsilon_{SS} \leq 0.05$ and $\kappa D_S \leq 1.0$, implying that the corresponding systems are effectively hyperuniform. Moreover, as T and κ decrease, H decreases, implying the increasing level of hyperuniformity for the corresponding system. For example, when we decrease k_BT/ε_{SS} to 0.01, the value of H falls below 10^{-3}. This is consistent with the fact that as κ decreases, the "screening" effect becomes weaker and the potential becomes longer-ranged. As a result, the suspension of charged colloids behaves more like the pure-Coulombic system in a neutralizing background, which is known to be perfectly

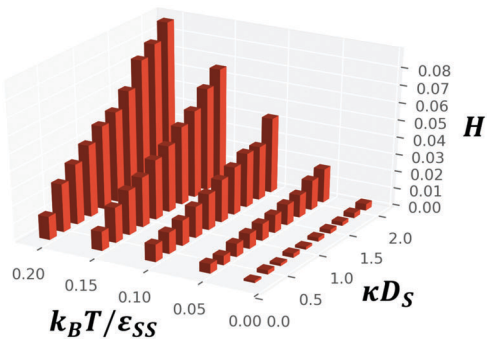

Fig. 4 Structural phase diagram of the "hyperuniformity index" in terms of the temperature T and inverse screening length κ constructed from 50 equilibrated systems of 5000 small and 5000 large charged colloids in a suspension with a small to large colloid diameter ratio α = 2/3 and a packing fraction ϕ of 0.21. H is on the order of 10^{-2}–10^{-3} when $k_BT/\varepsilon_{SS} \leq$ 0.05 and $\kappa D_S \leq$ 1.0, indicating that the corresponding systems are effectively hyperuniform. Moreover, as T and κ decrease, H decreases, implying the increasing level of hyperuniformity for the corresponding system.

hyperuniform.[26–28] Also, as T decreases, the system increasingly accesses lower energy states, in parallel with hard-core systems evolving towards lower enthalpy jammed states. As mentioned above, as hard-particle systems are driven towards jammed states, they tend to become hyperuniform.[23–25]

Last, we note that the configurations generated in our computer simulations could potentially be realized in experiments by depositing colloids onto solid substrates or at fluid interfaces[39–41] and allowing them to self-organize. Promising candidate colloids include polystyrene particles, proteins, and other macromolecules.[42–45] Note also that the hard-core component of our interactions can be experimentally modeled by grafting polymer chains to the surface of colloidal particles, minimizing the effect of attractive interactions.[46] In this connection, the set of parameters κ and ε_{ij} defining our interaction model can be approximately transformed into experimentally accessible/measurable quantities using the DLVO theory.[43,47] For instance, a binary mixture of colloids with Z_S = 150, Z_L = 367, D_S = 300 nm, and D_L = 450 nm (Z_S, Z_L, D_S, and D_L are charges and diameters of the small and large colloids, respectively) in an aqueous solution at 300 K, with its corresponding counter-ions and no other electrolytes present, roughly leads to $k_BT/\varepsilon_{SS} \approx 0.04$ and $\kappa D_S \approx 0.96$, and this system is predicted to be effectively hyperuniform. Once an experimental realization of the colloidal system on solid substrates or at fluid interfaces is obtained, snapshots of the configurations can then be taken by means of video optical microscopy, which can be further analyzed to check for hyperuniformity. Interested readers are referred to the work by Dreyfus and coworkers[48] for more detailed information on these issues. In addition, although in this work we focused on generating disordered hyperuniform materials in two dimensions through the self-structuring of binary mixtures of colloids in suspension, we expect that similar procedures can be applied to their three-dimensional counterparts, which might even have greater practical relevance.

Conclusions and discussion

In this work we proposed an approach to synthesize *in silico* two-dimensional disordered hyperuniform materials through the self-structuring (self-assembly) process of binary mixtures of charged colloids. Specifically, we systematically studied the small-wavenumber volume-fraction fluctuation behavior of a relatively large number of samples, probing the κ–T parameter space in search for effective hyperuniformity. In this way we have constructed a structural "phase diagram" of the "hyperuniformity index", H, in terms of T and κ. We have found that H reaches the order of 10^{-2}–10^{-3} when $k_BT/\varepsilon_{SS} \leq 0.05$ and $\kappa D_S \leq 1.0$, implying that the corresponding systems are effectively hyperuniform. Moreover, as the temperature and inverse screening length decrease (*i.e.* the concentration of counterions is lowered or the solvent's dielectric constant increases), H decreases, implying that the degree of hyperuniformity is augmented.

Our models could be translated into large laboratory samples at room temperature without resorting to the use of high pressures. As a comparison, a reduced pressure $P/(\rho k_BT)$ as high as 10^{11} is required to synthesize hyperuniform jammed systems, where P, ρ, and T are the pressure, number density, and temperature of the system, respectively.[25] Our findings provide a promising alternative to fabricate large samples of disordered hyperuniform two-phase systems for photonic and other applications.

In addition, we note that in the limit $\kappa \to 0$ and $r_C \to \infty$, the interaction in (3) becomes a bare Coulomb. From the findings of Lomba, Weis, and Torquato,[28] we know that in the limit our system will not reach strict multihyperuniformity, since it does not fulfill the required conditions, $\varepsilon_{ij} \neq \sqrt{\varepsilon_{ii}\varepsilon_{jj}}$, $\forall i \neq j$. In this work, we have shown that the system is also not multihyperuniform for nonzero κ. Finally, we note that while the present work focused on binary mixtures of charged colloids, it is straightforward to extend the analysis to charged mixtures with arbitrary size distributions and compositions.

Conflicts of interest

There are no conflicts to declare.

Acknowledgements

D. C. and S. T. were supported by the National Science Foundation under Award No. CBET-1701843. E. L. wishes to acknowledge the support from the Agencia Estatal de Investigación and Fondo Europeo de Desarrollo Regional (FEDER) under grant No. FIS2017-89361-C3-2-P, partial funding from the European Union's Horizon 2020 research and the innovation program under the Marie Sklodowska-Curie grant agreement No. 734276, and from the Program Salvador de Madariaga, PRX16/00069 which supported his sabbatical stay at the Chemistry Department of Princeton University.

References

1 S. Torquato and F. H. Stillinger, *Phys. Rev. E: Stat., Nonlinear, Soft Matter Phys.*, 2003, **68**, 041113.
2 C. E. Zachary and S. Torquato, *J. Stat. Mech.: Theory Exp.*, 2009, P12015.
3 S. Torquato, *Phys. Rep.*, 2018, **745**, 1–95.
4 S. Torquato, *J. Phys.: Condens. Matter*, 2016, **28**, 414012.
5 S. Torquato, *Phys. Rev. E*, 2016, **94**, 022122.
6 D. Chen and S. Torquato, *Acta Mater.*, 2018, **142**, 152–161.
7 Y. Xu, S. Chen, P. Chen, W. Xu and Y. Jiao, *Phys. Rev. E*, 2017, **96**, 043301.
8 R. A. DiStasio Jr, G. Zhang, F. H. Stillinger and S. Torquato, *Phys. Rev. E*, 2018, **97**, 023311.
9 M. Florescu, S. Torquato and P. J. Steinhardt, *Proc. Natl. Acad. Sci. U. S. A.*, 2009, **106**, 20658–20663.
10 W. Man, M. Florescu, E. P. Williamson, Y. He, S. R. Hashemizad, B. Y. C. Leung, D. R. Liner, S. Torquato, P. M. Chaikin and P. J. Steinhardt, *Proc. Natl. Acad. Sci. U. S. A.*, 2013, **110**, 15886–15891.
11 D. S. Wiersma, *Nat. Photonics*, 2013, **7**, 188.

12 G. Gkantzounis, T. Amoah and M. Florescu, *Phys. Rev. B*, 2017, **95**, 094120.
13 M. Hejna, P. J. Steinhardt and S. Torquato, *Phys. Rev. B: Condens. Matter Mater. Phys.*, 2013, **87**, 245204.
14 G. Zhang, F. H. Stillinger and S. Torquato, *J. Chem. Phys.*, 2016, **145**, 244109.
15 M. A. Klatt and S. Torquato, *Phys. Rev. E*, 2018, **97**, 012118.
16 O. Leseur, R. Pierrat and R. Carminati, *Optica*, 2016, **3**, 763–767.
17 L. S. Froufe-Pérez, M. Engel, J. J. Sáenz and F. Scheffold, *Proc. Natl. Acad. Sci. U. S. A.*, 2017, **114**, 9570–9574.
18 S. Yu, X. Piao, J. Hong and N. Park, *Nat. Commun.*, 2015, **6**, 8269.
19 T. Ma, H. Guerboukha, M. Girard, A. D. Squires, R. A. Lewis and M. Skorobogatiy, *Adv. Opt. Mater.*, 2016, **4**, 2085–2094.
20 M. Vaezi, H. Seitz and S. Yang, *Int. J. Adv. Des. Manuf. Technol.*, 2013, **67**, 1721–1754.
21 W. D. Piñeros, M. Baldea and T. M. Truskett, *J. Chem. Phys.*, 2016, **145**, 054901.
22 H. Pattabhiraman, G. Avvisati and M. Dijkstra, *Phys. Rev. Lett.*, 2017, **119**, 157401.
23 C. E. Zachary, Y. Jiao and S. Torquato, *Phys. Rev. Lett.*, 2011, **106**, 178001.
24 D. Chen and S. Torquato, *Phys. Rev. E: Stat., Nonlinear, Soft Matter Phys.*, 2015, **92**, 062207.
25 S. Atkinson, G. Zhang, A. B. Hopkins and S. Torquato, *Phys. Rev. E*, 2016, **94**, 012902.
26 J. L. Lebowitz, *Phys. Rev. A: At., Mol., Opt. Phys.*, 1983, **27**, 1491.
27 E. Lomba, J.-J. Weis and S. Torquato, *Phys. Rev. E*, 2017, **96**, 062126.
28 E. Lomba, J.-J. Weis and S. Torquato, *Phys. Rev. E*, 2018, **97**, 010102.
29 B. Derjaguin and L. Landau, *Appl. Sci. Res., Sect. B*, 1941, **14**, 633.
30 E. Verwey and J. Overbeek, *Theory of the Stability of Lyophobic Colloids*, Elsevier, Amsterdam, 1948.
31 S. Auer and D. Frenkel, *J. Phys.: Condens. Matter*, 2002, **14**, 7667.
32 A.-P. Hynninen and M. Dijkstra, *Phys. Rev. E: Stat., Nonlinear, Soft Matter Phys.*, 2003, **68**, 021407.
33 F. Martelli, S. Torquato, N. Giovambattista and R. Car, *Phys. Rev. Lett.*, 2017, **119**, 136002.
34 A. Chremos and J. F. Douglas, *Ann. Phys.*, 2017, **529**, 1600342.
35 Y. Jiao, T. Lau, H. Hatzikirou, M. Meyer-Hermann, J. C. Corbo and S. Torquato, *Phys. Rev. E: Stat., Nonlinear, Soft Matter Phys.*, 2014, **89**, 022721.
36 D. Frenkel and B. Smit, *Understanding Molecular Simulation: from Algorithms to Applications*, Academic Press, San Diego, CA, and London, 2001, vol. 1.
37 S. Torquato, *Random Heterogeneous Materials: Microstructure and Macroscopic Properties*, Springer, New York, 2002, vol. 16.
38 *Neutron, X-rays and Light. Scattering Methods applied to Soft Condensed Matter*, ed. P. Lindner and T. Zemb, North-Holland, Amsterdam, 2002.
39 D. Lombardo, M. A. Kiselev, S. Magazù and P. Calandra, *Adv. Condens. Matter Phys.*, 2015, **2015**, 151683.
40 Y. Yin, Y. Lu, B. Gates and Y. Xia, *J. Am. Chem. Soc.*, 2001, **123**, 8718–8729.
41 F. Reincke, S. G. Hickey, W. K. Kegel and D. Vanmaekelbergh, *Angew. Chem., Int. Ed.*, 2004, **43**, 458–462.
42 H. M. Lindsay and P. M. Chaikin, *J. Chem. Phys.*, 1982, **76**, 3774–3781.
43 R. O. Rosenberg, D. Thirumalai and R. D. Mountain, *J. Phys.: Condens. Matter*, 1989, **1**, 2109.
44 S. Magazu, G. Maisano, F. Mallamace and N. Micali, *Phys. Rev. A: At., Mol., Opt. Phys.*, 1989, **39**, 4195.
45 J. Gapinski, A. Wilk, A. Patkowski, W. Häussler, A. J. Banchio, R. Pecora and G. Nägele, *J. Chem. Phys.*, 2005, **123**, 054708.
46 E. P. K. Currie, W. Norde and M. A. C. Stuart, *Adv. Colloid Interface Sci.*, 2003, **100**, 205–265.
47 S. Sanyal and A. K. Sood, *Phys. Rev. E: Stat. Phys., Plasmas, Fluids, Relat. Interdiscip. Top.*, 1995, **52**, 4154.
48 R. Dreyfus, Y. Xu, T. Still, L. A. Hough, A. G. Yodh and S. Torquato, *Phys. Rev. E: Stat., Nonlinear, Soft Matter Phys.*, 2015, **91**, 012302.

